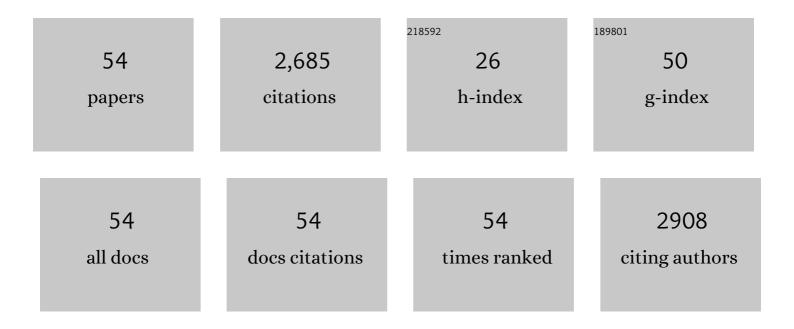


List of Publications by Year in descending order

Source: https://exaly.com/author-pdf/2553524/publications.pdf Version: 2024-02-01



#	Article	IF	CITATIONS
1	Single-element amorphous palladium nanoparticles formed via phase separation. Nano Research, 2022, 15, 5575-5580.	5.8	5
2	High figure-of-merit and power generation in high-entropy GeTe-based thermoelectrics. Science, 2022, 377, 208-213.	6.0	233
3	Electric Polarization Switching on an Atomically Thin Metallic Oxide. Nano Letters, 2021, 21, 144-150.	4.5	19
4	Coherent Sb/CuTe Core/Shell Nanostructure with Large Strain Contrast Boosting the Thermoelectric Performance of nâ€Type PbTe. Advanced Functional Materials, 2021, 31, 2007340.	7.8	30
5	SnSe, the rising star thermoelectric material: a new paradigm in atomic blocks, building intriguing physical properties. Materials Horizons, 2021, 8, 1847-1865.	6.4	29
6	Enhanced atomic ordering leads to high thermoelectric performance in AgSbTe ₂ . Science, 2021, 371, 722-727.	6.0	306
7	High-entropy-stabilized chalcogenides with high thermoelectric performance. Science, 2021, 371, 830-834.	6.0	546
8	Interfacial superstructures and chemical bonding transitions at metal-ceramic interfaces. Science Advances, 2021, 7, .	4.7	24
9	Significantly Enhanced Electrochemical Redox for Highâ€Performance Electrochemical Capacitor via Active Ionâ€Tunnel Oriented BaCoF ₄ Electrodes. Advanced Energy Materials, 2021, 11, 2003734.	10.2	4
10	Development and characterization of Nb3Sn/Al2O3 superconducting multilayers for particle accelerators. Scientific Reports, 2021, 11, 7770.	1.6	10
11	Entropy engineering promotes thermoelectric performance in p-type chalcogenides. Nature Communications, 2021, 12, 3234.	5.8	105
12	Modifying Li@Mn ₆ Superstructure Units by Al Substitution to Enhance the Long ycle Performance of Coâ€Free Liâ€Rich Cathode. Advanced Energy Materials, 2021, 11, 2101962.	10.2	39
13	Direct Atomic‣cale Structure and Electric Field Imaging of Triazineâ€Based Crystalline Carbon Nitride. Advanced Materials, 2021, 33, e2106359.	11.1	19
14	Rational design of D–ï€â€"D hole-transporting materials for efficient perovskite solar cells. Materials Chemistry Frontiers, 2021, 5, 7824-7832.	3.2	3
15	Porous Thermoelectric Zintl: YbCd ₂ Sb ₂ . ACS Applied Energy Materials, 2021, 4, 913-920.	2.5	9
16	Surface Crystallization of Amorphous Palladium Nanoparticles. Journal of Physical Chemistry C, 2021, 125, 1107-1112.	1.5	0
17	Interfacial Defect Passivation and Charge Carrier Management for Efficient Perovskite Solar Cells via a Highly Crystalline Small Molecule. ACS Energy Letters, 2021, 6, 4209-4219.	8.8	63
18	Watershed-scale distributions of heavy metals in the hyporheic zones of a heavily polluted Maozhou River watershed, southern China. Chemosphere, 2020, 239, 124773.	4.2	15

Lin Xie

#	Article	IF	CITATIONS
19	A highly asymmetric interfacial superstructure in WC: expanding the classic grain boundary segregation and new complexion theories. Materials Horizons, 2020, 7, 173-180.	6.4	26
20	Immobilization of Cr(VI) on engineered silicate nanoparticles: Microscopic mechanisms and site energy distribution. Journal of Hazardous Materials, 2020, 383, 121145.	6.5	18
21	Multilayer Ion Load and Diffusion on TMD/MXene Heterostructure Anodes for Alkali-Ion Batteries. ACS Applied Energy Materials, 2020, 3, 7699-7709.	2.5	22
22	Plasmonic evolution of atomically size-selected Au clusters by electron energy loss spectrum. National Science Review, 2020, 8, nwaa282.	4.6	5
23	Realizing Reduced Imperfections via Quantum Dots Interdiffusion in High Efficiency Perovskite Solar Cells. Advanced Materials, 2020, 32, e2003296.	11.1	50
24	Superconductivity in undoped BaFe ₂ As ₂ by tetrahedral geometry design. Proceedings of the National Academy of Sciences of the United States of America, 2020, 117, 21170-21174.	3.3	13
25	Constructing van der Waals gaps in cubic-structured SnTe-based thermoelectric materials. Energy and Environmental Science, 2020, 13, 5135-5142.	15.6	53
26	Magnetotransport signatures of Weyl physics and discrete scale invariance in the elemental semiconductor tellurium. Proceedings of the National Academy of Sciences of the United States of America, 2020, 117, 11337-11343.	3.3	42
27	Reduced NOM triggered rapid Cr(VI) reduction and formation of NOM-Cr(III) colloids in anoxic environments. Water Research, 2020, 181, 115923.	5.3	56
28	Atomic Imaging of Subsurface Interstitial Hydrogen and Insights into Surface Reactivity of Palladium Hydrides. Angewandte Chemie - International Edition, 2020, 59, 20348-20352.	7.2	36
29	Realizing Improved Thermoelectric Performance in Bil ₃ -Doped Sb ₂ Te ₃ (GeTe) ₁₇ via Introducing Dual Vacancy Defects. Chemistry of Materials, 2020, 32, 1693-1701.	3.2	36
30	Importance of Functional Groups in Cross-Linking Methoxysilane Additives for High-Efficiency and Stable Perovskite Solar Cells. ACS Energy Letters, 2019, 4, 2192-2200.	8.8	157
31	Superstructures: Directing Gold Nanoparticles into Freeâ€6tanding Honeycombâ€Like Ordered Mesoporous Superstructures (Small 31/2019). Small, 2019, 15, 1970165.	5.2	0
32	Intrinsic Conductance of Domain Walls in BiFeO ₃ . Advanced Materials, 2019, 31, e1902099.	11.1	39
33	Direct atomic-scale observation of the Ag ⁺ diffusion structure in the quasi-2D "liquid-like―state of superionic thermoelectric AgCrSe ₂ . Journal of Materials Chemistry C, 2019, 7, 9263-9269.	2.7	16
34	Direct Growth of Carbon Nanotubes Doped with Single Atomic Fe–N ₄ Active Sites and Neighboring Graphitic Nitrogen for Efficient and Stable Oxygen Reduction Electrocatalysis. Advanced Functional Materials, 2019, 29, 1906174.	7.8	159
35	Enhanced thermoelectric properties in chimney ladder structured Mn(BxSi1-x)1.75 due to the dual lattice occupation of boron. Applied Physics Letters, 2019, 115, 123902.	1.5	5
36	GaP–ZnS Multilayer Films: Visible-Light Photoelectrodes by Interface Engineering. Journal of Physical Chemistry C, 2019, 123, 3336-3342.	1.5	7

Lin Xie

#	Article	IF	CITATIONS
37	Chemical Bath Deposition of Coâ€Doped TiO ₂ Electron Transport Layer for Hysteresisâ€&uppressed Highâ€Efficiency Planar Perovskite Solar Cells. Solar Rrl, 2019, 3, 1900176.	3.1	36
38	Directing Gold Nanoparticles into Freeâ€Standing Honeycombâ€Like Ordered Mesoporous Superstructures. Small, 2019, 15, e1901304.	5.2	8
39	Deterministic Switching of Ferroelectric Bubble Nanodomains. Advanced Functional Materials, 2019, 29, 1808573.	7.8	30
40	High Thermoelectric Performance Achieved in GeTe–Bi ₂ Te ₃ Pseudoâ€Binary via Van der Waals Gapâ€Induced Hierarchical Ferroelectric Domain Structure. Advanced Functional Materials, 2019, 29, 1806613.	7.8	101
41	Elucidating the Role of Sulfide on the Stability of Ferrihydrite Colloids under Anoxic Conditions. Environmental Science & Technology, 2019, 53, 4173-4184.	4.6	31
42	Step-Up Thermoelectric Performance Realized in Bi ₂ Te ₃ Alloyed GeTe via Carrier Concentration and Microstructure Modulations. ACS Applied Energy Materials, 2019, 2, 1616-1622.	2.5	25
43	Feâ€Nâ€C Catalysts: Direct Growth of Carbon Nanotubes Doped with Single Atomic Fe–N ₄ Active Sites and Neighboring Graphitic Nitrogen for Efficient and Stable Oxygen Reduction Electrocatalysis (Adv. Funct. Mater. 49/2019). Advanced Functional Materials, 2019, 29, 1970332.	7.8	3
44	Formation and stability of NOM-Mn(III) colloids in aquatic environments. Water Research, 2019, 149, 190-201.	5.3	64
45	Colossal photovoltages in strain-driven crystal field transition and symmetry breaking of superconducting epitaxial systems. Physical Review Materials, 2019, 3, .	0.9	1
46	Efficient and Reproducible CH ₃ NH ₃ PbI ₃ Perovskite Layer Prepared Using a Binary Solvent Containing a Cyclic Urea Additive. ACS Applied Materials & Interfaces, 2018, 10, 9390-9397.	4.0	31
47	Control of Epitaxial BaFe ₂ As ₂ Atomic Configurations with Substrate Surface Terminations. Nano Letters, 2018, 18, 6347-6352.	4.5	16
48	Energetics of Nanoparticle Exsolution from Perovskite Oxides. Journal of Physical Chemistry Letters, 2018, 9, 3772-3778.	2.1	65
49	Enhanced Bidimensionalityâ€Driven Ultrahigh Laserâ€Induced Voltages in Highâ€ <i>T</i> _c Superconducting Epitaxial Films. Advanced Electronic Materials, 2018, 4, 1800116.	2.6	11
50	Ternary solvent for CH ₃ NH ₃ PbI ₃ perovskite films with uniform domain size. Physical Chemistry Chemical Physics, 2017, 19, 1143-1150.	1.3	29
51	Organic Photovoltaics Utilizing a Polymer Nanofiber/Fullerene Interdigitated Bilayer Prepared by Sequential Solution Deposition. Journal of Physical Chemistry C, 2016, 120, 12933-12940.	1.5	18
52	Effective protection of sequential solution-processed polymer/fullerene bilayer solar cell against charge recombination and degradation. Organic Electronics, 2015, 25, 212-218.	1.4	12
53	ZnS-GaP Solid Solution Thin Films with Enhanced Visible-Light Photocurrent. ACS Applied Energy Materials, 0, , .	2.5	4
54	Preparation and magnetic properties of cylindrical permalloy nanowire arrays. MRS Communications, 0, , 1.	0.8	1